catalysts

MDPI

Article

The Reaction Mechanism of Acetaldehyde Ammoximation to Its Oxime in the TS-1/H_2O_2 System

Chaoqun Meng [1,2], Suohe Yang [1], Guangxiang He [1], Guohua Luo [1], Xin Xu [1] and Haibo Jin [1,*]

[1] Department of Chemical Engineering, Beijing Institute of Petrochemical Technology, Beijing 102617, China; m362077142@163.com (C.M.); yangsuohe@bipt.edu.cn (S.Y.); hgx@bipt.edu.cn (G.H.); luoguohua@bipt.edu.cn (G.L.); xuxin@bipt.edu.cn (X.X.)

[2] College of Chemical Engineering, Beijing University of Chemical Technology, Beijing 100029, China

* Correspondence: jinhaibo@bipt.edu.cn; Tel.: +86-184-1822-9069

Academic Editor: Keith Hohn

Received: 11 May 2016; Accepted: 16 July 2016; Published: 22 July 2016

Abstract: A qualitative analysis for the ammoximation of acetaldehyde to its oxime in the TS-1(Titanium Silicalite-1)/H_2O_2 system was investigated using an in situ infrared spectrometer (ReactIR15). NH_3 is first oxidized to NH_2OH by TS-1/H_2O_2; then, CH_3CH=NOH forms after NH_2OH reacts with CH_3CHO. That means the intermediate of this reaction is NH_2OH instead of CH_3CH=NH. Experiments have been conducted to verify the mechanism, and the results are in good agreement with the infrared findings.

Keywords: TS-1; H_2O_2; ReactIR15; ammoximation; acetaldehyde

1. Introduction

Acetaldoxime is one of the simplest oxime-containing compounds, and it has a wide variety of uses in chemical synthesis processes as an important intermediate [1,2]. It is especially notable for its commercial application as an intermediate in the production of pesticides and cyanogenic glucosides [3] or as boiler chemicals to remove oxygen with its limited toxicity and strong reduction [2]. Initially, acetaldoxime can be prepared using hydroxylamine sulfate or hydroxylamine hydrochloride with sodium nitrite and sulfur dioxide, which has a low utilization rate, a high level of low value by-products and serious environmental pollution effects [4–6]. Therefore, it is extremely important to develop a new synthesis process for acetaldoxime. Acetaldehyde ammoximation to its oxime using TS-1 (Titanium Silicalite-1) as a catalyst and H_2O_2 as an oxidant offers a better approach [7–10]. Moreover, the utilization of carbon atoms is up to 100%, and water is a unique byproduct [11] that meets the development requirements of green chemical industry [12–14].

Due to its excellent performance, the TS-1/H_2O_2 system has been widely used in the hydroxylation of benzene, ammoxidation of ketone and epoxidation of alkenes, etc. Wang et al. investigated the correlation between the membrane structure and reaction efficiency; additionally, the effects of the conditions on the benzene conversion, product yield, hydrogen conversion and water production rate were examined in detail [15]. Somnath Nandi et al. evaluated the efficacy of the hybrid formalism for modeling and optimizing the zeolite (TS-1)-catalyzed benzene hydroxylation to phenol reaction whereby several sets of optimized operating conditions were obtained [16]. Tsai et al. reported the effects of the TS-1 crystal size and post-treatment on the porous structure and catalytic performances of TS-1 in phenol hydroxylation [17]. Liu et al. investigated the influences of essential process parameters on ammoximation and the reaction conditions [18]. Jiang et al. developed a new approach for phenol production by one-step selective hydroxylation of benzene with hydrogen peroxide over an ultrafine TS-1 in a submerged ceramic membrane reactor [19]. Li et al. investigated the feasibility of continuous ammoximation of acetone to acetone oxime over TS-1, and the effects of operation

conditions were examined in the tubular membrane reactor [20]. Bars et al. made comparisons between TS-1, Ti-A1-Beta and Ti-ZSM-48 in the liquid-phase ammoximation of cyclohexanone [21]. Sang Baek Shin and David Chadwick studied the kinetics of the heterogeneous catalytic epoxidation of propene in the TS-1/H_2O_2 system and reported on the apparent activation energy [22]. V. Russo et al. performed a kinetic investigation of both the main and side reactions, aiming to find general kinetic expressions and related parameters in the reaction of propene oxide production via hydrogen peroxide with TS-1 [23]. Jernej Stare assessed various aspects of propene epoxidation using hydrogen peroxide and then elucidated some of the important factors that govern its mechanism [24].

Most researchers studied the reaction conditions, catalysis preparation, catalytic performance and more. In addition, some researchers considered the mechanism of the TS-1/H_2O_2 system. However, until now, only two main reaction amination mechanisms have been proposed. One is the hydroxylamine pathway; its intermediate is hydroxylamine, such that NH_3 is first oxidized to hydroxylamine by H_2O_2 on the site of Ti. Then, hydroxylamine reacts with reagent, forming a target product. Sirijaraensre and Limtrakul illustrated the presence of hydroxylamine in the liquid phase using adsorption microcalorimetry IR, XANES and EXAFS techniques, as well as DFT (Density Functional Theory) calculations with the ONIOM scheme [25]. Chu et al. demonstrated that Ti-OOH is the oxidant in the TS-1/H_2O_2 system and that the formation of NH_2OH passed through a lower reaction energy barrier according to Gibbs free energies and DFT [26]. Pozzo et al. used an experimental approach instead of calculating the values to explain the existence of hydroxylamine by determining the nitrate and nitrite concentrations [27].

The other mechanism is the imine pathway. In this pathway, NH_3 reacts with reagent via TS-1, forming imine, which is then oxidized to a target product with the collective effect of H_2O_2 and TS-1. Zhang et al. studied the ammoximation of cyclohexanone with H_2O_2 and NH_3 on TS-1 using DRIFTS and concluded that the peroxytitano complex—Ti-OOH was formed after TS-1 was treated with H_2O_2. Additionally, it reacted with imine to produce oxime [28]. Tvarłžková et al. analyzed the adsorption of ammonia and cyclohexanone on TS-1 according to the IR spectra and observed the presence of cyclohexylimine [29]. In addition, Yip and Hu suggested the two proposed reaction models using kinetic analysis, namely, the Langmuir-Hinshelwood (LH) and Eley-Rideal (ER) mechanisms [30]. Liu et al. proposed a new possible mechanism in which the intermediate had strong absorption of the C–O bond with the aid of on-line ATR–FTIR spectroscopy [31]. However, most articles did not clearly describe the catalytic mechanism in the TS-1/H_2O_2 System. Thangaraj et al. reported the possible mechanisms for the formation of oxime, including the imine and hydroxylamine pathways [32]. Xia et al. demonstrated that hydrogen peroxide could be adsorbed and activated at the Ti sites of TS-1 by combing DFT calculations with experimental studies [33]. Bolis et al. also computed the absorption of ammonia on TS-1 using adsorption micro calorimetry IR, XANES and EXAFS techniques, and the authors showed that a minor level of ammonia was irreversibly held at the TS-1 surface [34]. Zecchina et al. clarified the structure of the titanium silicon molecular sieve at different reaction times and reported on the presence of an intermediate TS-1 structure, $(\equiv SiO)_3(H_2O)_2TiOOH$, with IR, Raman, UV-Vis and XAFS spectroscopy methods [35]. Zhang et al. inferred that acetone, butanone, cyclohexanone and 3-methylcyclohexanone could enter the TS-1 cavity, which was not the case for 4-butylcyclohexanone with TGA (Thermal Gravity Analysis) [36].

From the above reviews, it is very complex and difficult to study the mechanism of ammoximation in the TS-1/H_2O_2 system through the reaction between acetaldehyde and its oxime. In the area of theoretical study, we used an in-situ infrared spectrometer (ReactIR15, METTLER-TOLEDO, Zurich, Switzerland). FTIR is an effective way to identify substances and analyze the structure of the material, and it is now commonly used. However, this method still has some shortcomings. First, it is troublesome to make the sample with solid compression and a liquid membrane. Moreover, it is possible to cause morphological changes or surface contamination when adding infrared inert material or making the self-support tablet. This results in concealing the true nature of the material. Inconveniently, the instrument can only detect the substance off-line. Because it cannot track changes

in the reaction system, we cannot see the entire reaction process. ReactIR15, which was utilized in this paper, can support a scanning liquid-phase reaction and instantly generate infrared spectrum results. ReactIR15 can analyze the material on-line without damaging the material. Based on the analysis of the characteristic peaks, we can identify whether a specific substance is present and then perform qualitative analysis of the reaction mechanism. On the basis of the experimental analysis, we conducted the experiments, and some useful information was obtained from the comparison of the two reaction mechanism pathways. We illustrated the mechanism using two approaches, and the results were mutually supportive and complementary.

2. Results and Discussion

2.1. Analysis of Imine Reaction Mechanism

Ammonia, acetaldehyde and TS-1 were added to the reactor in accordance with the order of reactants with a constant proportion under agitation conditions. Then, hydrogen peroxide was added after all peaks visible on the computer stabilized (see Figure 1). To eliminate overlapping peaks, the characteristic peaks were processed.

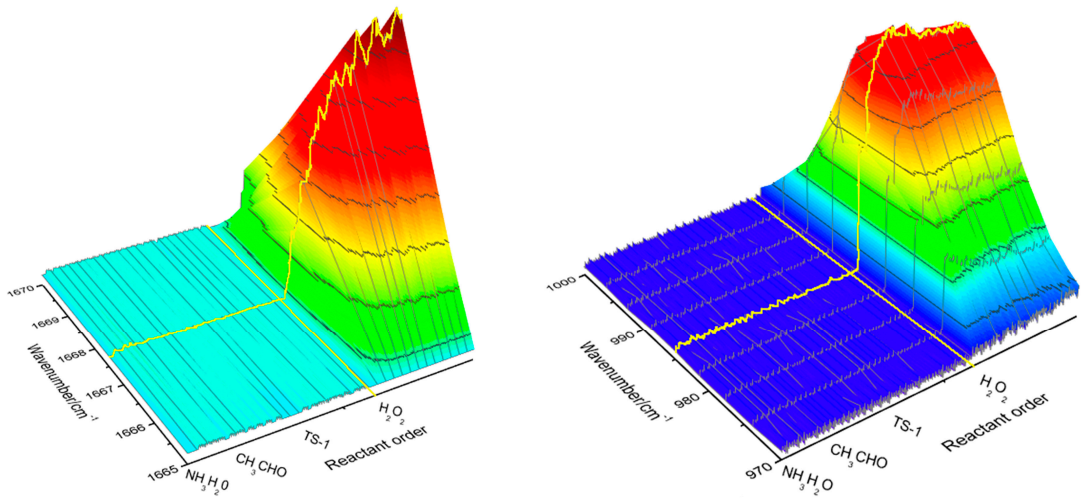

(**a**) (**b**)

Figure 1. With the addition of reactants in order, (**a**) the peak value of 1667 cm^{-1} and (**b**) the peak value of 985 cm^{-1} changed.

As in Figure 1, there was no absorption peak near 1670 cm^{-1} without hydrogen peroxide. However, the C=N bond stretching vibration absorption peak appeared at 1667 cm^{-1} after hydrogen peroxide was added; additionally, the peak intensity was high, and the peak increased rapidly. At the same time, there was an N–O bond absorption peak at 985 cm^{-1}, indicating that there was no intermediate product containing a C=N bond; instead, acetaldehyde imine was formed. Additionally, the C=N and N–O absorption peaks coalesced after the addition of hydrogen peroxide, which showed that acetaldoxime is generated.

2.2. Analysis of Hydroxylamine Reaction Mechanism

Ammonia, hydrogen peroxide and TS-1 were added to the reactor in a guaranteed proportion under agitation conditions. Additionally, acetaldehyde was added after all peaks visible on the computer stabilized (see Figure 2). Similarly, all peaks were separated to avoid overlap with each other.

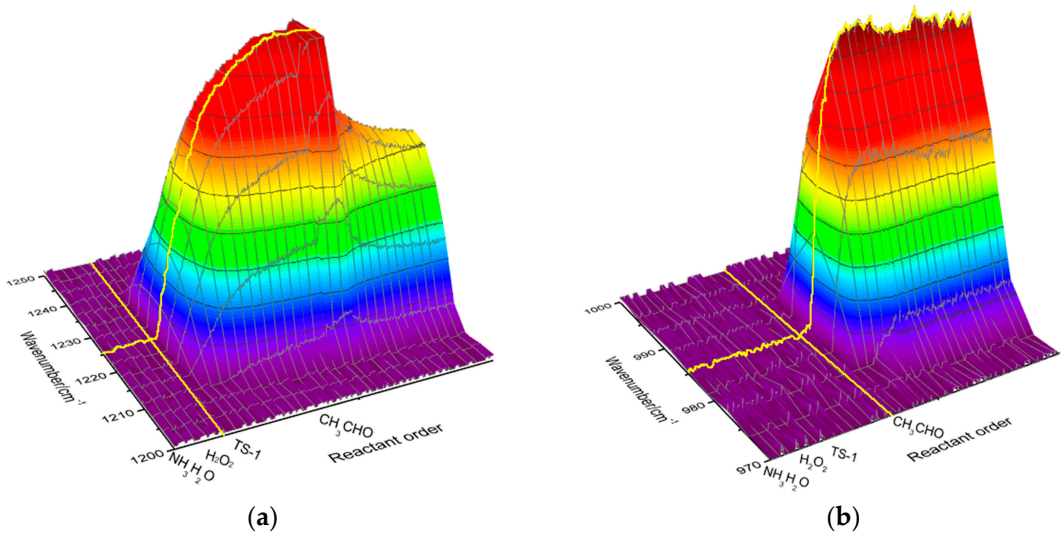

Figure 2. With the reactants added in the same order, (**a**) peak curve at 1227 cm^{-1} and (**b**) Peak curve at 985 cm^{-1} began to change in a different pattern.

As in Figure 2, the specific peak of hydroxylamine at 1227 cm^{-1} was significantly higher after the addition of TS-1, indicating hydroxylamine was generated. After the peak stabilized, the peak at 1227 cm^{-1} gradually decreased with the addition of acetaldehyde, and a peak at 985 cm^{-1} attributed to oxime simultaneously appeared. This indicated that acetaldehyde was formed after the addition of acetaldehyde. However, the peak value of 1227 cm^{-1} was not reduced to the original one before the addition of TS-1, which may be caused by catalytic activity, reaction conditions and other reasons and may lead to incomplete transformation of hydroxylamine to oxime. Based on Figure 2, we can conclude that hydroxylamine was generated and then formed acetaldoxime throughout the reaction process.

2.3. The Comparative Test and Results

Based on the above infrared results, we designed experiments to confirm the mechanism. The entire reaction was divided into two steps. First, ammonia reacted with hydrogen peroxide in the presence of TS-1. Second, the reaction solution was filtered off TS-1 and then continued to react with acetaldehyde. Additionally, the reaction with TS-1 in two steps was performed as a contrast experiment.

In the above two groups of experiments, the acetaldehyde selectivity was similar, but it was not high. The acetaldehyde conversion rate was much lower than the contrasting experiment for the design experiment in Figure 3.

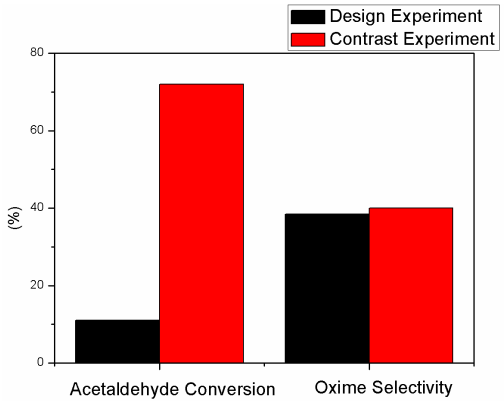

Figure 3. Comparison of the two groups of experimental results.

The acetaldehyde solutions were analyzed by LC-MS and GC-MS. We found many byproducts in the system, which were identified as self-condensation products of acetaldehyde in Figure 4. Although many substances cannot be precisely identified, we could make conclusions that these byproducts contributed to the low acetaldoxime selectivity. Monitoring the hydroxylamine concentration using ReactIR15, we found that the hydroxylamine concentration was uniformly reduced during filtration. This is because hydroxylamine is generated in the TS-1 channels by catalysis and was transferred into the reaction solution. Because of the excess ammonia in the system, the solution was alkaline. However, in an alkalescent environment, hydroxylamine is extremely unstable, and it is easily decomposed into ammonia, nitrogen, nitrate and water [37–40]. After the addition of acetaldehyde in the second step, the hydroxylamine concentration decreased rapidly to a low value. Then, it remained stable, as in Figure 5. Because of the decomposition of hydroxylamine, there was a much lower concentration that reacted with acetaldehyde in the design experiment compared to the contrasting one, which led to the low conversion rate of acetaldehyde. The entire progress is presented in Figure 6. These results demonstrated that the procedure for generating hydroxylamine was the control step of the reaction. Moreover, the second step is a non-catalytic reaction such that the entire reaction passes through hydroxylamine.

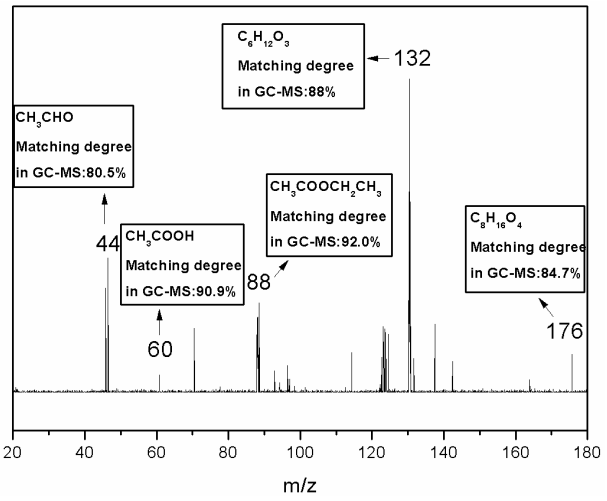

Figure 4. The comprehensive results of acetaldehyde in GC-MS and LC-MS.

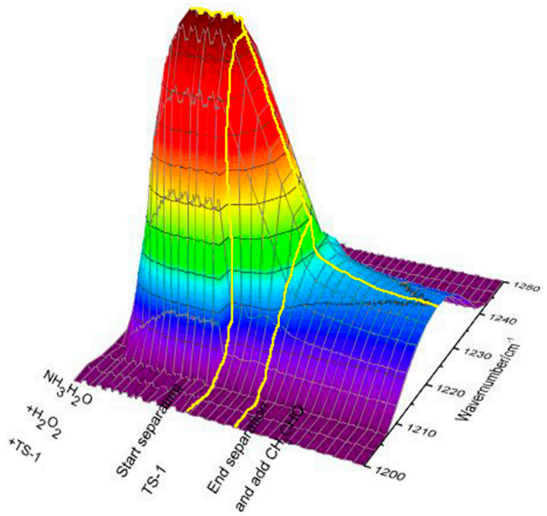

Figure 5. The change of the peak value of hydroxylamine in the entire process of the design experiment, including the separation step of the catalyst.

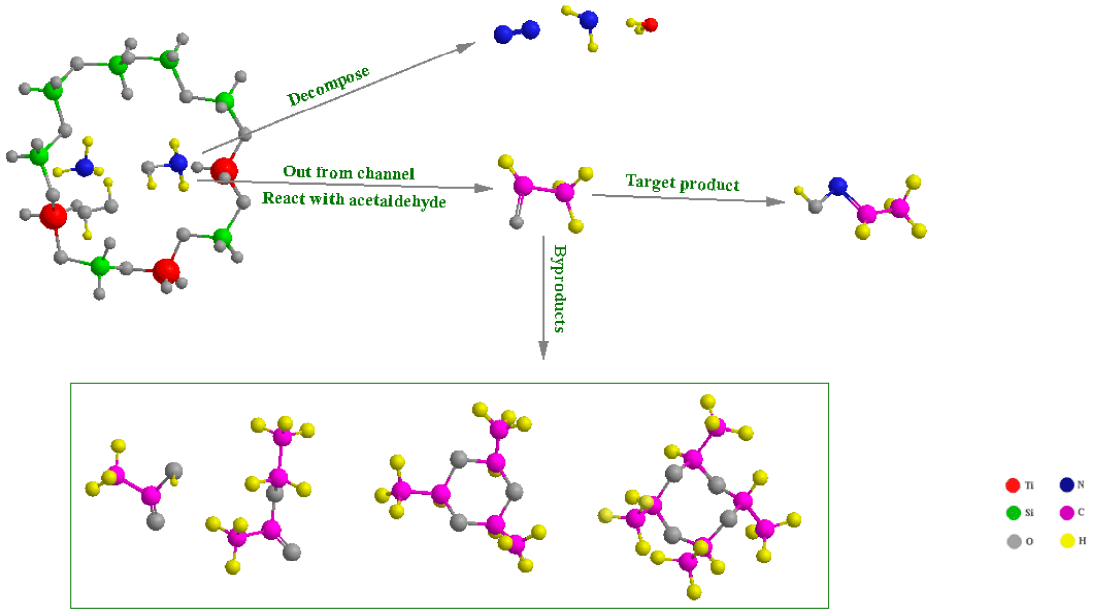

Figure 6. In the TS-1/H_2O_2 system, the reaction pathway of acetaldehyde ammoximation to acetaldehyde and the byproducts are presented in the experiments.

3. Experimental

3.1. Materials and Measurements

The industrial catalyst TS-1 (average particle size of approximately 0.2 μm; surface area of 417 $m^2 \cdot g^{-1}$) was provided by RIPP, SINOPEC. Analytical grade ammonia (25%, AR, Sinopharm, Shanghai, China), hydrogen peroxide (30%, AR, Sinopharm, ShangHai, China), acetaldehyde (40%, AR, GuangFu, Tianjin, China), hydroxylamine hydrochloride (98.5%, AR, GuangFu, Tianjin, China) and acetaldoxime (HPLC, TCI, Tokyo, Japan) were all obtained commercially. Acetaldehyde was purified by distillation and stored at 0 °C.

The GC-2014C (SHIMADZU, Tokyo, Japan) was equipped with a TCD detector. The packed column (3 m × 4 mm × 0.25 mm) was filled with 10% PEG6000, which was applied to the 101 pickling white diatomite carrier, and the oven temperature was kept at 100 °C. H_2 was used as carrier gas at a flow rate of 55 mL· min^{-1}. The detector temperature was 120 °C and injection port temperature was 140 °C. The injection quantity was 0.4 μL.

GC-MS analysis was accomplished using a gas chromatograph/mass spectrometer (7890A GC/5975C MS, Agilent, CA, USA). The separation column for GC-MS was DB-5MS (30 m × 0.25 mm × 0.25 μm). Helium was used as a carrier gas with a flow rate of 1.0 mL min^{-1}. The oven temperature was initially 40 °C and kept for 2 min. Then, it increased to 290 °C at a rate of 4 °C· min^{-1} and was kept for 4 min. The injection port temperature was 280 °C.

LC-MS analysis was achieved using a liquid chromatograph/mass spectrometer (Alianle2695+2Q2000, Waters, Milford, MA, USA). Liquid chromatographic separation was optimized and established on a reverse phase ODSC18 column (150 mm × 2.1 mm × 5 μm), which was kept at room temperature, and the mobile phase was acetonitrile-water solution (80:20). The flow rate was 0.2 mL· min^{-1}, and the detection wavelength was 254 nm. Mass spectrometer detection and quantification were performed in negative mode. The curtain gas was 0.5 MPa and the ion spray voltage was 35 V. The scanning range was 20–180 m/z, and the dryer flow rate was 500 L· min^{-1}.

A ReactIR15 reaction analysis system (METTLER-TOLEDO, Zurich, CHE, Switzerland, 2012), equipped with a light conduit and diamond insertion probe, was used to collect the mid-FTIR spectra of the condensation components. Additionally, the system of MCT (Mercury cadmium telluride) was

cooled using liquid nitrogen. FTIR spectra were collected in the wave number range between 3000 and 650 cm^{-1}.

3.2. Experimental Procedures

We obtained the infrared spectrum of aldehyde, deionized water, ammonia, acetaldoxime and hydroxylamine using ReactIR15. The experiments were performed at 60 °C in a 250-mL, four-necked flask with a condenser, thermometer, and magnetic stirrer. The molar ratio of each substance was CH_3CHO:H_2O_2:NH_3 = 1:1:2.5. The acetaldehyde level was 0.1 mol, and H_2O_2 was added using a micro pump for 30 min at a rate of 0.14 mL· min^{-1}. The catalyst amount was 0.5 g. The ReactIR15 probe was stretched into the liquid system and scanned every 15 s. The experimental device is shown in Figure 7. The addition order of the reactants according to the separate mechanisms of imine and hydroxylamine are listed as follows (as shown in Figure 8).

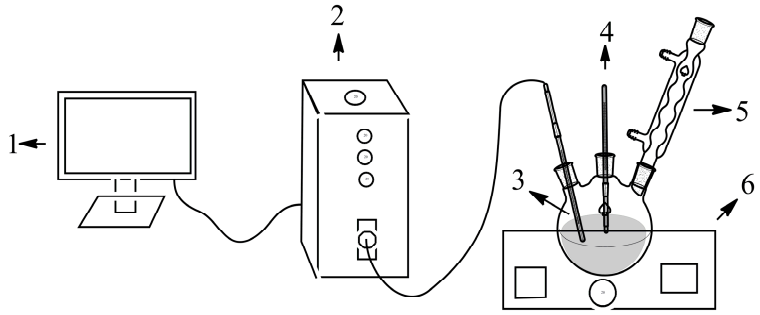

Figure 7. Diagram of the experiment setup; 1. Data analysis of computer; 2. ReactIR15; 3. Dector part; 4. Electric mixer; 5. Reflux condensation; 6. Oil bath pot.

The sequence of reactants in hydroxylamine mechanism

$$NH_3H_2O \xrightarrow[\text{stability}]{\text{Peak}} + H_2O_2\ (\text{by pumping}) \xrightarrow[\text{stability}]{\text{Peak}} + \text{TS-1} \xrightarrow[\text{stability}]{\text{Peak}} + CH_3CHO$$

The sequence of reactants in imine mechanism

$$NH_3H_2O \xrightarrow[\text{stability}]{\text{Pcak}} + CH_3CHO \xrightarrow[\text{stability}]{\text{Peak}} + \text{TS-1} \xrightarrow[\text{stability}]{\text{Peak}} + H_2O_2\ (\text{by pumping})$$

Figure 8. The different sequences of reactants in two mechanisms.

3.3. Spectral Analysis

To analyze the typical IR spectra of hydroxylamine and acetaldoxime, the absorption band of C=N bond in acetaldoxime is located at 1667 cm^{-1}, and the N–O bond stretching vibration absorption is a strong band, which is located between 1055 and 870 cm^{-1} and sometimes split into a few peaks.

Because the 2250–1950 cm^{-1} region for the diamond is the infrared shielding area, we selected approximately 1670 cm^{-1} as the C=N bond stretching vibration absorption peak and 985 cm^{-1} as the N–O bond absorption peak by comparing to the pure material infrared spectrum. Both characteristic peaks of the acetaldoxime absorption are shown in Figure 9a. In addition, we similarly chose 1220 cm^{-1} as a characteristic peak of hydroxylamine in Figure 9b.

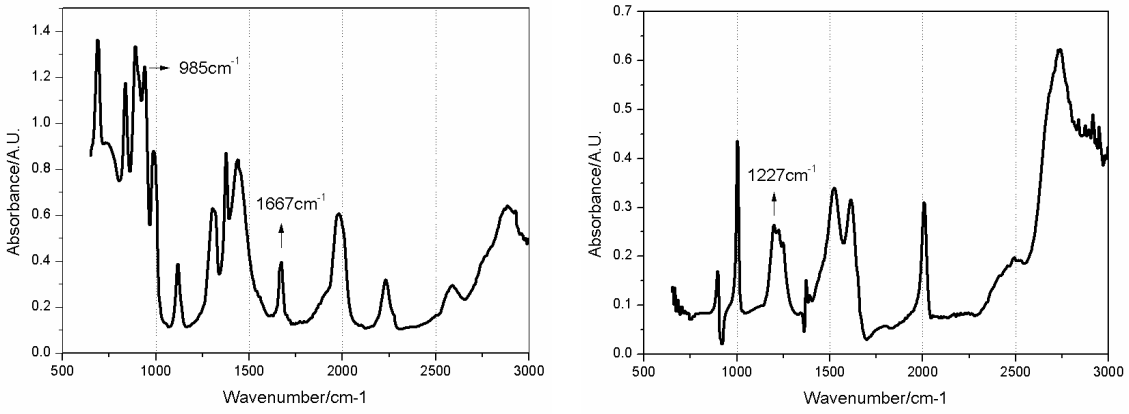

(**a**) (**b**)

Figure 9. The infrared spectrum of pure substances acquired by ReactIR15: (**a**) IR spectrum of acetaldoxime and (**b**) IR spectrum of hydroxylamine.

4. Conclusions

Based on the experimental results of the infrared spectrum and two step reactions, we can confirm that the hydroxylamine route may be the most important catalytic mechanism for the liquid phase ammoximation of acetaldehyde to its oxime in the TS-1/H_2O_2 system by the appearance of the hydroxylamine infrared characteristic peak. At the same, the experiments confirmed that the process by which hydroxylamine reacts with acetaldehyde was a non-catalytic reaction. Furthermore, hydroxylamine is confirmed to be the intermediate in the reaction of ammoximation with TS-1 in the liquid phase. However, this work is not completely finished. In the future, we can also explain the reaction mechanism according to the dynamics and more or less achieve a quantitative determination of the intermediate products.

Acknowledgments: This research was supported by the National Natural Science Foundation of China under agreement number 21073020, and The Importation and Development of High-Caliber Talents Project of Beijing Municipal Institutions Agreement Number CIT&TCD 20130325.

Author Contributions: C.M., S.Y. and H.J. conceived and designed the experiments; C.M. performed the experiments; C.M., G.L. and X.X. analyzed the data; G.H. contributed materials; C.M. and H.J. wrote the paper.

Conflicts of Interest: The authors declare no conflict of interest.

References

1. Kim, S.; Kim, H. An efficient Pd-catalyzed hydration of nitrile with acetaldoxime. *Tetrahedron Lett.* **2009**, *50*, 2973–2975. [CrossRef]
2. Ma, X.; He, Y. Copper (II)-catalyzed hydration of nitriles with the aid of acetaldoxime. *Tetrahedron Lett.* **2012**, *53*, 449–452. [CrossRef]
3. Soledade, M.; Sabine, P. Probing Crucial Metabolic Pathways in Fungal Pathogens of Crucifers: Biotransformation of Indole-3-Acetaldoxime, 4-Hydroxyphenylacetaldoxime, and Their Metabolites. *Bioorg. Med. Chem.* **2003**, *11*, 3115–3120.
4. Shi, H.; Guo, H. Experiment of acetaldehyde oxime being reducer in boiler acid cleaning. *Clean. World* **2007**, *23*, 10–12.
5. Shuo, Z.; Xiu, D. Ammoximation of citronellal with H_2O_2 catalyzed by TS-1. *Chin. J. Catal.* **2012**, *33*, 723–729.
6. Aurelia, V.; Alina, M. A new route for the synthesis of titanium silicalite-1. *Mater. Res. Bull.* **2012**, *17*, 35–41.
7. Wang, Y.; Zhang, S. The mechanism of catalyst deactivation and by-product formation in acetone ammoximation catalyzed by hollow titanium silicalite. *J. Mol. Catal. A Chem.* **2014**, *385*, 1–6. [CrossRef]
8. Wu, Y. Improve on the synthesis method of acetaldoxime. *Chem. Adhes.* **2005**, *01*, 61–62.

9. Yi, Z.; Xiang, W. Synthesis of titanium silicalite-1 with small crystal size by using mother liquor of titanium silicalite-1 as seeds (II): Influence of synthesis conditions on properties of titaniumsilicalite-1. *Microporous Mesoporous Mater.* **2012**, *162*, 105–114.
10. Qiang, L.; Gang, L. Synthesis of hierarchical TS-1 with convenient separation and the application for the oxidative desulfurization of bulky and small reactants. *Fule* **2014**, *130*, 70–75.
11. Romano, U.; Esposito, A. Selective Oxidation with Ti-Silicalite. *Stud. Surf. Sci. Catal.* **1990**, *55*, 33–41.
12. Liu, X.; Wang, X. Effect of solvent on the propylene epoxidation over TS-1 catalyst. *Catal. Today* **2004**, *93–95*, 505–509. [CrossRef]
13. Kwon, S.; Schweitzer, N. A kinetic study of vapor-phase cyclohexene epoxidation by H_2O_2 over mesoporous TS-1. *J. Catal.* **2015**, *326*, 107–115. [CrossRef]
14. Chen, R.; Bu, Z. Scouring-ball effect of microsized silica particles on operation stability of the membrane reactor for acetone ammoximation over TS-1. *Chem. Eng. J.* **2010**, *156*, 418–422. [CrossRef]
15. Wang, X.; Meng, B. Direct Hydroxylation of Benzene to Phenol Using Palladium–Titanium Silicalite Zeolite Bifunctional Membrane Reactors. *Ind. Eng. Chem. Res.* **2014**, *53*, 5636–5645. [CrossRef]
16. Nandi, S.; Mukherjee, P. Reaction Modeling and Optimization Using Neural Networks and Genetic Algorithms: Case Study Involving TS-1-Catalyzed Hydroxylation of Benzene. *Ind. Eng. Chem. Res.* **2002**, *41*, 2159–2169. [CrossRef]
17. Tsai, S.; Chao, P. Effects of pore structure of post-treated TS-1 on phenol hydroxylation. *Catal. Today* **2009**, *148*, 174–178. [CrossRef]
18. Liu, G.; Wu, J. Ammoximation of Cyclohexanone to Cyclohexanone Oxime Catalyzed by Titanium Silicalite-1 Zeolite in Three-phase System. *Chin. J. Chem. Eng.* **2012**, *20*, 889–894. [CrossRef]
19. Jiang, H.; She, F. One-step Continuous Phenol Synthesis Technology via Selective Hydroxylation of Benzene over Ultrafine TS-1 in a Submerged Ceramic Membrane Reactor. *Chin. J. Chem. Eng.* **2014**, *22*, 1199–1207. [CrossRef]
20. Li, Z.; Chen, R. Continuous Acetone Ammoximation over TS-1 in a Tubular Membrane Reactor. *Ind. Eng. Chem. Res.* **2010**, *49*, 6309–6316. [CrossRef]
21. Bars, J.; Dakka, J. Ammoximation of cyclohexanone and hydroxyaromatic ketones over titanium molecular sieves. *Appl. Catal. A Gen.* **1996**, *136*, 69–80. [CrossRef]
22. Shin, S.; Chadwick, D. Kinetics of Heterogeneous Catalytic Epoxidation of Propene with Hydrogen Peroxide over Titanium Silicalite (TS-1). *Ind. Eng. Chem. Res.* **2010**, *49*, 8125–8134. [CrossRef]
23. Russo, V.; Tesser, R. Kinetics of Propene Oxide Production via Hydrogen Peroxide with TS-1. *Ind. Eng. Chem. Res.* **2014**, *53*, 6274–6287. [CrossRef]
24. Stare, J.; Neil, J. Mechanistic Aspects of Propene Epoxidation by Hydrogen Peroxide. Catalytic Role of Water Molecules, External Electric Field, and Zeolite Framework of TS-1. *J. Chem. Inf. Model.* **2009**, *49*, 833–846. [CrossRef] [PubMed]
25. Jakkapan, S.; Jumras, L. Mechanisms of the ammonia oxidation by hydrogen peroxide over the perfect and defective Ti species of TS-1 zeolite. *Phys. Chem. Chem. Phys.* **2013**, *15*, 18093–18100.
26. Chang, C.; Hai, Z. Density functional theory studies on hydroxylamine mechanism of cyclohexanone ammoximation on titanium silicalite-1 catalyst. *J. Mol. Model.* **2013**, *19*, 2217–2224.
27. Pozzo, L.; Fornasari, G. TS-1 catalytic mechanism in cyclohexanone oxime production. *Catal. Commun.* **2002**, *3*, 369–375. [CrossRef]
28. Xiang, Z.; Rui, M. In-situ FTIR study on mechanism of cyclohexanone ammoximation to its oxime on TS-1 in liquid phase. *J. Hebei Univ. Sci. Technol.* **2011**, *06*, 605–610.
29. Tvarłžková, Z.; Habersberger, K.; Žilkova, N.; Jírł, P. Role of surface complexes on titanium-silicate in the ammoximation of cyclohexanone with hydrogen peroxide. *Appl. Catal. A Gen.* **1991**, *79*, 105–114. [CrossRef]
30. Alex, C.; Xi, H. Catalytic Activity of Clay-Based Titanium Silicalite-1 Composite in Cyclohexanone Ammoximation. *Ind. Eng. Chem. Res.* **2009**, *48*, 8441–8450.
31. Liu, H.; Liu, P. Studies on the liquid-phase ammoximation of cyclohexanone over a titanium silicate sieve using on-line ATR–FTIR spectroscopy. *Catal. Commun.* **2010**, *11*, 887–891. [CrossRef]
32. Thangaraj, A.; Sivasanker, S. Catalytic Properties of Crystalline Titanium Silicalites III. Ammoximation of Cyclohexanone. *J. Catal.* **1991**, *131*, 394–400. [CrossRef]
33. Chang, X.; Long, J. Heterogeneous oxidation of cyclohexanone catalyzed by TS-1: Combined experimental and DFT studies. *Chin. J. Catal.* **2015**, *36*, 845–854.

34. Bolis, V.; Bordiga, S. A calorimetric, IR, XANES and EXAFS study of the adsorption of NH_3 on Ti-silicalite as a function of the sample pre-treatment. *Microporous Mesoporous Mater.* **1999**, *30*, 67–76. [CrossRef]
35. Zecchina, A.; Bordiga, S. Structural characterization of Ti centres in Ti-silicalite and reaction mechanisms in cyclohexanone ammoximation. *Catal. Today* **1996**, *32*, 97–106. [CrossRef]
36. Yong, Z.; Ya, W. Reaction mechanism of the ammoximation of ketones catalyzed by TS-1. *React. Kinet. Catal. Lett.* **2006**, *87*, 25–32.
37. Le, X.; Jiang, D. Distinctions of hydroxylamine formation and decomposition in cyclohexanone ammoximation over microporous titanosilicates. *J. Catal.* **2014**, *309*, 1–10. [CrossRef]
38. Adamopoulou, T.; Manolis, K. Thermal decomposition of hydroxylamine: Isoperibolic calorimetric measurements at different conditions. *J. Hazard. Mater.* **2013**, *254–255*, 382–389. [CrossRef] [PubMed]
39. Adamopoulou, T.; Papadaki, M. Use of isoperibolic calorimetry for the study of the effect of water concentration, temperature and reactor venting on the rate of hydroxylamine thermal decomposition. *J. Loss Prev. Process Ind.* **2012**, *25*, 803–808. [CrossRef]
40. Liu, L.; Papadaki, M. Isothermal decomposition of hydroxylamine and hydroxylamine nitrate in aqueous solutions in the temperature range 80–160 °C. *J. Hazard. Mater.* **2009**, *165*, 573–578. [CrossRef] [PubMed]